IEEE Access
Multidisciplinary | Rapid Review | Open Access Journal

Received April 26, 2018, accepted May 22, 2018, date of publication May 28, 2018, date of current version June 26, 2018.

Digital Object Identifier 10.1109/ACCESS.2018.2841010

PMU-Based Estimation of Voltage-to-Power Sensitivity for Distribution Networks Considering the Sparsity of Jacobian Matrix

PENG LI[1], (Member, IEEE), HONGZHI SU[1], CHENGSHAN WANG[1], (Senior Member, IEEE), ZHELIN LIU[1], AND JIANZHONG WU[2], (Member, IEEE)

[1]Key Laboratory of Smart Grid of Ministry of Education, Tianjin University, Tianjin 300072, China
[2]School of Engineering, Institute of Energy, Cardiff University, Cardiff CF24 3AA, U.K.

Corresponding author: Chengshan Wang (cswang@tju.edu.cn)

This work was supported by the National Key Research and Development Program of China under Grant 2017YFB0902900 and Grant 2017YFB0902902.

ABSTRACT With increasing integration of various distributed energy resources, electric distribution networks are changing to an energy exchange platform. Accurate voltage-to-power sensitivities play a vital role in system operation and control. Relative to the off-line method, measurement-based sensitivity estimation avoids the errors caused by incorrect device parameters and changes in network topology. An online estimation of the voltage-to-power sensitivity based on phasor measurement units is proposed. The sparsity of the Jacobian matrix is fully used by reformulating the original least-squares estimation problem as a sparse-recovery problem via compressive sensing. To accommodate the deficiency of the existing greedy algorithm caused by the correlation of the sensing matrix, a modified sparse-recovery algorithm is proposed based on the mutual coherence of the phase angle and voltage magnitude variation vectors. The proposed method can ensure the accuracy of estimation with fewer measurements and can improve the computational efficiency. Case studies on the IEEE 33-node test feeder verify the correctness and effectiveness of the proposed method.

INDEX TERMS Smart distribution network, voltage-to-power sensitivity, compressive sensing, phasor measurement units.

I. INTRODUCTION

The increasing penetration of distributed generators (DGs), flexible loads and energy storage poses new challenges to the operation and dispatch of distribution networks, requiring substantial improvements in system observability and controllability [1]–[3]. Reverse power flow and harmonic pollution are challenging traditional management and protection technologies [4]. Distribution networks are more prone to congestions and voltage problems [5], [6]. Therefore, the distribution system operator (DSO) must have fast and accurate access to the current status and its evolution in the near future [7]. To effectively manage the uncertainties associated with both demand and generation, it is critical to precisely acquire the sensitivities of operation state variables to the fluctuation of loads and renewables [8], [9]. Conventionally, the voltage-to-power sensitivities are obtained from the power flow calculation. The accuracy is not guaranteed since the results depend heavily on accurate line parameters and up-to-date network topology which may not always be available [10].

To accommodate the DGs and flexible loads, the need for monitoring and analysis of distribution system behavior in real time is growing. However, the existing supervisory control and data acquisition (SCADA) system cannot readily meet the need for precision and real-time performance [11]. Phasor measurement units (PMUs) can achieve high-precision synchronous measurements [12] and are applied both in electric transmission systems and distribution systems. Their application can effectively improve the system observability and provide new options to address the challenges in operation control [13]. Certain micro-synchrophasors (μPMUs) have been exploited for distribution system operational control to improve the performance of the electric power distribution and coordination [14]. μPMUs can support the control of distributed energy resources. With lower cost and smaller size, μPMUs can meet the economic

requirements of distribution utilities. Their applications in fault detection, model validation, and state estimation were evaluated in [15]. The high-resolution measurements of the voltage phase angle can offer significant new options for actively managing distribution systems.

The accuracy of state estimation is greatly improved with the help of measurements from PMU in [16]. Furthermore, considering the line parameter errors, PMU measurements can be used in state estimation to identify the erroneous transmission line parameters in [17]. Least-squares estimation (LSE) is used to estimate the parameters of the branches that are PMU-observable. Line parameters are estimated directly from PMU data at the two ends via total least-squares estimation (TLSE) in [18] to accommodate measurement errors. With the buses monitored all equipped with PMUs, sensitivity parameters of the complete system can be estimated in the power transmission system [19], [20]. Linear sensitivity distribution factors were computed from multi-time slot PMU data based on LSE in [21]. A statistical admittance matrix estimation approach was proposed in [22] based on PMU data via cross-correlation analysis. Power flow Jacobian matrix was estimated using LSE via the vectors of active power, reactive power, phase angle and voltage magnitude variations obtained from real-time and historical PMU data in [23]. These sensitivity parameter estimation methods depend entirely on the measurements, meaning that inaccuracies in the line parameters and topology information have no effect on the estimation results.

In the present study, the voltage-to-power sensitivities are obtained from the inversion of the estimated power flow Jacobian matrix. Differing from the preliminary work, we exploit a sparse representation of the Jacobian matrix estimation. The sparsity was also used in [24] and [25] to estimate the transmission system distribution factors and nodal-admittance matrix. The accuracy of estimation is improved considerably. However, unlike transmission systems, real and reactive power flows cannot be decoupled in distribution networks; thus, their linear approximations are invalid. To exploit the sparsity, the original LSE problem is transformed into a sparse-recovery problem via compressive sensing (CS). An exact solution of the CS reconstruction problem directly from the minimization of the l_0 norm is unpractical as this approach requires an exhaustive combinatorial search [26]. Greedy algorithms such as orthogonal matching pursuit (OMP) are effective ways to find approximate solutions in constrained error tolerance [27]. To guarantee the efficiency of finding the candidate solution that is sufficiently sparse, the restrict isometry property (RIP) is required which needs lower coherence between the columns of the sensing matrix [27]. However, the sensing matrix of the power flow Jacobian matrix estimation is composed of the vectors of phase angle and voltage magnitude variations. These vectors are highly correlated, which adversely affects the convergence of the existing greedy algorithms.

Here, we present an online method to estimate the voltage-to-power sensitivity considering the sparsity of the power flow Jacobian matrix. The main contributions of this study are as follows: 1) The sparsity of the power flow Jacobian matrix is exploited in estimation. A sparse-recovery model of the Jacobian matrix estimation is proposed via compressive sensing. The demands of effective measurements are highly reduced while ensuring estimation accuracy. 2) The correlation in the sensing matrix is used to improve the performance of the existing greedy algorithm. Coherence-based compressive sampling match pursuit (CohCoSaMP) is proposed to accommodate the deficiency of the existing greedy algorithm caused by the correlation of the sensing matrix and enhance the convergence.

The remainder of this paper is organized as follows. Section II describes the PMU-based power flow Jacobian matrix estimation problem based on LSE method. In Section III, the LSE problem is transformed into a sparse-recovery problem via compressive sensing, and CohCoSaMP is proposed to solve the problem effectively. In Section IV, case studies on IEEE 33-node test feeder verify the validity of the proposed algorithm. The conclusions are drawn in Section V.

II. ESTIMATION OF THE POWER FLOW JACOBIAN MATRIX BASED ON PMU MEASUREMENTS

A. DEFINITION OF THE POWER FLOW JACOBIAN MATRIX

By linearizing the nonlinear power flow equation at the current operation point, the relationship of power variation and voltage variation can be expressed as shown in (1).

$$\begin{bmatrix} \Delta \boldsymbol{P} \\ \Delta \boldsymbol{Q} \end{bmatrix} = \begin{bmatrix} \boldsymbol{H} & \boldsymbol{N} \\ \boldsymbol{M} & \boldsymbol{L} \end{bmatrix} \begin{bmatrix} \Delta \boldsymbol{\theta} \\ \Delta \boldsymbol{V} \end{bmatrix} = \boldsymbol{J} \begin{bmatrix} \Delta \boldsymbol{\theta} \\ \Delta \boldsymbol{V} \end{bmatrix} \tag{1}$$

where $\Delta \boldsymbol{P}$ and $\Delta \boldsymbol{Q}$ denote the change of active power and reactive power at each node, respectively. $\Delta \boldsymbol{\theta}$ and $\Delta \boldsymbol{V}$ denote the change of phase angle and voltage magnitude at each node, respectively. $\boldsymbol{J}$ is the Jacobian matrix of the power flow equation in the current state. $\boldsymbol{H}$, $\boldsymbol{N}$, $\boldsymbol{M}$, and $\boldsymbol{L}$ are the submatrices of $\boldsymbol{J}$, and the elements are partial derivatives of active and reactive power with respect to phase angle and voltage magnitude as follows.

$$\begin{aligned} H_{ij} &= \partial P_i / \partial \theta_j, \quad N_{ij} = \partial P_i / \partial V_j, \\ M_{ij} &= \partial Q_i / \partial \theta_j, \quad \text{and } L_{ij} = \partial Q_i / \partial V_j. \end{aligned}$$

B. APPROXIMATE LINEAR RELATIONSHIP BETWEEN VARIATIONS OF VOLTAGE AND POWER

Let $\Delta P_i^{\theta_j}$ denote the change in active power injection at node i caused by a small variation of the phase angle at node j, denoted by $\Delta \theta_j$. Then, the relationship can be expressed as shown in (2).

$$H_{ij} = \partial P_i / \partial \theta_j \approx \Delta P_i^{\theta_j} / \Delta \theta_j \tag{2}$$

Suppose that $\Delta P_i^{V_j}$ denotes the change in active power injection at node i due to a small variation of voltage magnitude at node j, expressed as ΔV_j. Then, the following relation can be obtained.

$$N_{ij} = \partial P_i / \partial V_j \approx \Delta P_i^{V_j} / \Delta V_j \tag{3}$$

Therefore, the change of active power can be expressed as the sum of variations resulting from the change of phase angle and voltage magnitude at each node. Then, the change of active power at node i, denoted by ΔP_i, can be described as shown in (4).

$$\Delta P_i = \sum\nolimits_{j\in\Omega}\left(\Delta P_i^{\theta_j} + \Delta P_i^{V_j}\right) \tag{4}$$

where Ω denotes the set of nodes in the distribution network.

By substituting (2) and (3) into (4), the relationship of the active power change of PQ nodes and PV nodes with the phase angle and voltage magnitude change can be approximated as shown in (5).

$$\Delta P_i \approx \sum\nolimits_{j\in\Omega_{\mathrm{L}}\cup\Omega_{\mathrm{V}}} H_{ij}\Delta\theta_j + \sum\nolimits_{j\in\Omega_{\mathrm{L}}} N_{ij}\Delta V_j \tag{5}$$

where Ω_{L} denotes the set of PQ nodes, Ω_{V} denotes the set of PV nodes.

Similarly, as shown in (6), the relationship of the reactive power change of PQ nodes to the phase angle and voltage magnitude change can be approximated by the elements of the Jacobian matrix.

$$\Delta Q_i \approx \sum\nolimits_{j\in\Omega_{\mathrm{L}}\cup\Omega_{\mathrm{V}}} M_{ij}\Delta\theta_j + \sum\nolimits_{j\in\Omega_{\mathrm{L}}} L_{ij}\Delta V_j \tag{6}$$

C. PMU-BASED JACOBIAN MATRIX ESTIMATION

The historical measurements of PMU for analysis can be acquired via a phasor data concentrator (PDC) [30]. However, because of the high frequency of measurements, the operation state change in the measurement time step may be too small to be used in sensitivity estimation. Let $P_i(t), Q_i(t), \theta_i(t)$ and $V_i(t)$ denote the current measurements of active power, reactive power, phase angle and voltage magnitude at node i, respectively. The measurements of the current operation point of node i are expressed as $P_i[0] = P_i(t), Q_i[0] = Q_i(t), \theta_i[0] = \theta_i(t)$, and $V_i[0] = V_i(t)$. Let $P_i(t - m\Delta t), Q_i(t - m\Delta t), \theta_i(t - m\Delta t)$, and $V_i(t - m\Delta t)$ represent the m^{th} history measurements of node i. To ensure effective measurement, the distance between the m^{th} historical time step and the current operation point is defined as shown in (7).

$$D_{m,0} = \sqrt{\sum\nolimits_{i\in\Omega}(\Delta P_i(m,0)/S_{\mathrm{B}})^2 + \sum\nolimits_{i\in\Omega}(\Delta Q_i(m,0)/S_{\mathrm{B}})^2} \tag{7}$$

where Δt is the time step of the measurements. $\Delta P_i(m,0) = P_i(t - m\Delta t) - P_i[0]$, and $\Delta Q_i(m,0) = Q_i(t - m\Delta t) - Q_i[0]$. S_{B} denotes the rated capacity. α is defined as the threshold value of operation state judgement. If $D_{m,0} \le \alpha$, then the m^{th} time step is regarded as the same operation point of the current state; otherwise, for $D_{m,0} > \alpha$ and for any $p < m$ that satisfies $D_{p,0} \le \alpha$, then the m^{th} time step is regarded as the first group historical operation point, and for the $(m+1)^{\mathrm{th}}$ time step, its distance with the first group historical operation point, denoted by $D_{m+1,1}$, is calculated to find a new historical operation point. This process continues until C groups of historical measurements are obtained to meet the estimation requirements. Suppose that $P_i[k]$, $Q_i[k], \theta_i[k]$, and $V_i[k]$ denote the active power, reactive power, phase angle and voltage magnitude of the k^{th} historical operation point of node i, respectively. The corresponding flow chart to obtain the effective PMU measurements is shown in Fig. 1.

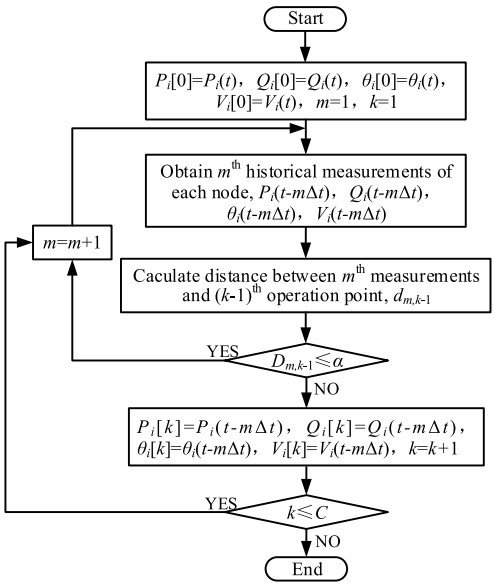

FIGURE 1. Flow chart to obtain the effective PMU measurements.

Then C groups of variations of power and voltage are obtained by subtracting each group historical measurement from the current measurement.

$$\begin{aligned}\Delta P_i[k] &= P_i[k] - P_i[0]\\ \Delta Q_i[k] &= Q_i[k] - Q_i[0]\\ \Delta\theta_i[k] &= \theta_i[k] - \theta_i[0]\\ \Delta V_i[k] &= \theta_i[k] - \theta_i[0]\end{aligned}$$

where $k = 1, 2, \cdots, C$. According to (5) and (6), the approximate linear relationships are obtained as shown in (8) and (9).

$$\Delta P_i[k] \approx \sum\nolimits_{j\in\Omega_{\mathrm{L}}\cup\Omega_{\mathrm{V}}} H_{ij}\Delta\theta_j[k] + \sum\nolimits_{j\in\Omega_{\mathrm{L}}} N_{ij}\Delta V_j[k] \tag{8}$$

$$\Delta Q_i[k] \approx \sum\nolimits_{j\in\Omega_{\mathrm{L}}\cup\Omega_{\mathrm{V}}} M_{ij}\Delta\theta_j[k] + \sum\nolimits_{j\in\Omega_{\mathrm{L}}} L_{ij}\Delta V_j[k] \tag{9}$$

For node i, the variation vectors of power and voltage are interpreted as follows.

$$\begin{aligned}\Delta\boldsymbol{P}_i &= [\Delta P_i[1], \cdots, \Delta P_i[C]]^T,\\ \Delta\boldsymbol{Q}_i &= [\Delta Q_i[1], \cdots, \Delta Q_i[C]]^T,\\ \Delta\boldsymbol{\theta}_i &= [\Delta\theta_i[1], \cdots, \Delta\theta_i[C]]^T,\\ \Delta\boldsymbol{V}_i &= [\Delta V_i[1], \cdots, \Delta V_i[C]]^T,\end{aligned}$$

When $C > 2|\Omega_{\mathrm{L}}| + |\Omega_{\mathrm{V}}|$, the following overdetermined equations are formulated.

$$\Delta\boldsymbol{P}_i \approx \begin{bmatrix}(\Delta\boldsymbol{\theta}_j)_{j\in\Omega_{\mathrm{L}}\cup\Omega_{\mathrm{V}}} & (\Delta\boldsymbol{V}_j)_{j\in\Omega_{\mathrm{L}}}\end{bmatrix}\begin{bmatrix}\boldsymbol{H}_i^T\\ \boldsymbol{N}_i^T\end{bmatrix} \tag{10}$$

$$\Delta\boldsymbol{Q}_i \approx \begin{bmatrix}(\Delta\boldsymbol{\theta}_j)_{j\in\Omega_{\mathrm{L}}\cup\Omega_{\mathrm{V}}} & (\Delta\boldsymbol{V}_j)_{j\in\Omega_{\mathrm{L}}}\end{bmatrix}\begin{bmatrix}\boldsymbol{M}_i^T\\ \boldsymbol{L}_i^T\end{bmatrix} \tag{11}$$

where $\boldsymbol{H}_i = \left[(H_{ij})_{j\in\Omega_L\cup\Omega_V}\right]$, $\boldsymbol{N}_i = \left[(N_{ij})_{j\in\Omega_L}\right]$, $\boldsymbol{M}_i = \left[(M_{ij})_{j\in\Omega_L\cup\Omega_V}\right]$ and $\boldsymbol{L}_i = \left[(L_{ij})_{j\in\Omega_L}\right]$ denote the i^{th} row of each submatrix of the power flow Jacobian matrix. $|\Omega_L|$ is the cardinality of Ω_L, and $|\Omega_V|$ is the cardinality of Ω_V.

The LSE problem is modeled as (12) with the sensing matrix $\tilde{\boldsymbol{A}} = \left[\left(\Delta\boldsymbol{\theta}_j\right)_{j\in\Omega_L\cup\Omega_V}\left(\Delta\boldsymbol{V}_j\right)_{j\in\Omega_L}\right]$.

$$\begin{aligned}&\min\ \boldsymbol{e}_{i,\mathrm{P}}^T\boldsymbol{e}_{i,\mathrm{P}}\\&\text{s.t. } \Delta\boldsymbol{P}_i = \tilde{\boldsymbol{A}}\begin{bmatrix}\boldsymbol{H}_i^T\\ \boldsymbol{N}_i^T\end{bmatrix} + \boldsymbol{e}_{i,\mathrm{P}}\end{aligned} \tag{12}$$

where $\boldsymbol{e}_{i,\mathrm{P}}$ denotes the residual vector of active power of node i.

By solving the LSE problem (12), the optimal estimates of $\boldsymbol{H}_i$ and $\boldsymbol{N}_i$ are given by (13).

$$\begin{bmatrix}\hat{\boldsymbol{H}}_i^T\\ \hat{\boldsymbol{N}}_i^T\end{bmatrix} = \left(\tilde{\boldsymbol{A}}^T\tilde{\boldsymbol{A}}\right)^{-1}\tilde{\boldsymbol{A}}^T\Delta\boldsymbol{P}_i \tag{13}$$

where $\hat{\boldsymbol{H}}_i$ is the estimation of $\boldsymbol{H}_i$ and $\hat{\boldsymbol{N}}_i$ is the estimation of $\boldsymbol{N}_i$.

In the same way, the optimal estimates of $\boldsymbol{M}_i$ and $\boldsymbol{L}_i$ can be acquired.

III. VOLTAGE-TO-POWER SENSITIVITY ESTIMATION CONSIDERING THE SPARSITY OF THE JACOBIAN MATRIX

It is necessary to formulate overdetermined equations to estimate the power flow Jacobian matrix, which means that the sets of effective measurements must be greater than the dimensions of the linear equation. However, the Jacobian matrix is a sparse matrix according to the power flow equations, as shown in (14) and (15). The nonzero elements of each row arise only in the position corresponding to the directly connected nodes.

$$P_i = V_i\sum\nolimits_{j\in\Omega_i} V_j\left(G_{ij}\cos\theta_{ij} + B_{ij}\sin\theta_{ij}\right) \tag{14}$$

$$Q_i = V_i\sum\nolimits_{j\in\Omega_i} V_j\left(G_{ij}\sin\theta_{ij} - B_{ij}\cos\theta_{ij}\right) \tag{15}$$

where P_i and Q_i denote the active and reactive power injecting node i, respectively. V_i and V_j denote the voltage magnitudes of node i and node j, respectively. $\theta_{ij} = \theta_i - \theta_j$ denotes the phase angle difference between node i and node j. Ω_i denotes the set of nodes directly connected to node i. G_{ij} and B_{ij} denote the conductance and susceptance, respectively, between nodes i and j.

A. SPARSE REPRESENTATION OF JACOBIAN MATRIX ESTIMATION

Set $\boldsymbol{x} = \begin{bmatrix}\boldsymbol{H}_i^T\\ \boldsymbol{N}_i^T\end{bmatrix}$ and $\boldsymbol{y} = \Delta\boldsymbol{P}_i$. By normalizing matrix $\tilde{\boldsymbol{A}}$, a new sensing matrix $\boldsymbol{A}$ is acquired. The elements of $\boldsymbol{A}$ satisfy the relationship as follows.

$$A_{i,j} = \tilde{A}_{i,j}/\left\|\tilde{\boldsymbol{A}}_j\right\|_2 \tag{16}$$

where $\|\cdot\|_2$ denotes the l_2 norm. Then, we obtain the following relationship.

$$\boldsymbol{y} \approx \boldsymbol{A}\boldsymbol{x} \tag{17}$$

Furthermore, the following sparse-recovery problem is obtained by taking the sparsity of vector $\boldsymbol{x}$ into account.

$$\begin{aligned}&\min\ \|\boldsymbol{x}\|_0\\&\|\boldsymbol{y} - \boldsymbol{A}\boldsymbol{x}\|_2 \le\varepsilon\end{aligned} \tag{18}$$

where $\|\cdot\|_0$ denotes the l_0 norm. ε is a user-specified error tolerance that may depend on the level of measurement noise expected from the PMU data. The value of ε can be set according to the value of measurement variation vector $\boldsymbol{y}$ which is obtained from the PMU data. With the influence of the measurement errors and linear hypothesis of the relation between the variation of power and voltage, the value of $\|\boldsymbol{y} - \boldsymbol{A}\boldsymbol{x}\|_2$ cannot be zero, even if the actual value of $\boldsymbol{x}$ is obtained in the iteration of the method. Therefore, ε can be set as a relative error tolerance of $\|\boldsymbol{y} - \boldsymbol{A}\boldsymbol{x}\|_2$ to $\|\boldsymbol{y}\|_2$. When the relative error is small enough, it is considered that the optimal approximation is obtained.

B. GREEDY ALGORITHMS FOR SPARSE RECOVERY

As it is unfeasible to solve (18) directly, basis pursuit (BP) algorithms [31] and greedy pursuit algorithms [32] have been developed to find approximate solutions to (18). Relative to the convex relaxation method, greedy algorithms have merits in both accuracy and computational complexity [33]. OMP is the most commonly used greedy algorithm to solve the sparse-recovery problem [34]; its flowchart is given in Algorithm 1, where λ_n denotes the selected column index of the sensing matrix in the n^{th} iteration. $\boldsymbol{r}_n$ is the residual vector in the n^{th} iteration. N is the column number of the sensing matrix. $\boldsymbol{A}_j$ denotes the j^{th} column of matrix $\boldsymbol{A}$. Λ_n denotes the index set of sensing matrix column number in n^{th} iteration. $\boldsymbol{A}_{\Lambda_n}$ is the matrix composing the columns of the sensing matrix corresponding to the set Λ_n. $\hat{\boldsymbol{x}}_{\Lambda_n}$ is a vector composed of the elements of $\hat{\boldsymbol{x}}$ corresponding to set Λ_n.

OMP selects only one column of the sensing matrix in the index set in each iteration and thus requires many iterations and copious computation time to solve the problem. If the sparsity level is K, regularized orthogonal matching pursuit (ROMP) improves OMP by selecting K columns into the index set in each iteration and introducing a regularization rule that reduces not only the times of iteration but also the number of columns selected [35]. Compressive sampling matching pursuit (CoSaMP) introduces an additional pruning step to refine the estimate recursively. CoSaMP retains only $2K$ components of the index set that corresponding to the $2K$ largest-magnitude components of the LSE solution [36]. In contrast to the two previous algorithms, CoSaMP can remove the invalid candidates from index set, thus reducing the size of the final index set and improving the accuracy of estimation.

Algorithm 1 OMP [34]

Input: sensing matrix $\boldsymbol{A}$, observations $\boldsymbol{y}$, threshold value of estimation error ε, maximum iterations M

Output: estimated value $\hat{\boldsymbol{x}}$ of sparse vector $\boldsymbol{x}$

Initialize: residual $\boldsymbol{r}_0 = \boldsymbol{y}$, index set of the sensing matrix column number $\Lambda_0 = \emptyset$, iteration $n = 1$ $\hat{\boldsymbol{x}} = \boldsymbol{0}$

1. Select the column of sensing matrix that has the highest inner product with residual.

$$\lambda_n = \text{argmax}_{j=1:N} \left| \left\langle \boldsymbol{r}_{n-1}, \boldsymbol{A}_j \right\rangle \right| \tag{19}$$

2. Update the index set Λ_n.

$$\Lambda_n = \Lambda_{n-1} \bigcup \{\lambda_n\} \tag{20}$$

3. Solve the LSE problem.

$$\hat{\boldsymbol{x}}_n = \left(\boldsymbol{A}_{\Lambda_n}^T \boldsymbol{A}_{\Lambda_n} \right)^{-1} \boldsymbol{A}_{\Lambda_n}^T \boldsymbol{y} \tag{21}$$

4. Update the residual $\boldsymbol{r}_n$.

$$\boldsymbol{r}_n = \boldsymbol{y} - \boldsymbol{A}_{\Lambda_n} \hat{\boldsymbol{x}}_n \tag{22}$$

5. Continue to step 6 if $n > M$ or $\|\boldsymbol{r}_n\|_2 < \varepsilon$; otherwise, set $n = n + 1$ and return to step 1.
6. Obtain the solution $\hat{\boldsymbol{x}}$ according to $\hat{\boldsymbol{x}}_n$.

$$\hat{\boldsymbol{x}}_{\Lambda_n} = \hat{\boldsymbol{x}}_n \tag{23}$$

C. COHERENCE-BASED CoSaMP

The efficiency of existing greedy algorithms for sparse-recovery depends on the sensing matrix satisfying the restrict isometry property that is the columns of the sensing matrix have relatively low coherence with each other [37]. However, the columns of the sensing matrix of the Jacobian matrix estimation, composed of the vectors of the phase angle and voltage magnitude variations, are highly correlated with each other. Therefore, the existing OMP-type algorithm cannot guarantee the convergence and accuracy of the estimation.

Coherence in the sensing matrix is harmful to the convergence of the greedy pursuit algorithm, but the vectors of phase angle and voltage magnitude variations of directly connected nodes typically have a higher coherence with each other than with other nodes. The nonzero elements of each row appear in the position that corresponds exactly to the directly connected nodes. Therefore, we can select several columns into the index set that have the highest correlation with the corresponding phase angle and voltage magnitude variations as initial candidates to improve the efficiency of the algorithm.

CohCoSaMP is proposed to extend CoSaMP in estimating the Jacobian matrix of the power flow equation. According to (14) and (15), the relationship between the number of nonzero elements, denoted by K_i, corresponding to the node i and the degree of node i, is $K_i = 2(d_i + 1)$. We first estimate the maximal degree of the nodes in the distribution network. Then, $2(d_{\max} + 1)$ columns of sensing matrix that have the highest coherence with the phase angle and voltage magnitude variations of node i are selected to form the index set. The LSE solution is obtained according to the index set. The final estimation is obtained if the estimation error is less than the threshold value. Otherwise, the number of elements in the index set is extended. The $4(d_{\max} + 1)$ columns of the sensing matrix are transferred into the index set according to the coherence. A CoSaMP process is activated if the algorithm still does not converge. The complete flowchart of CohCoSaMP is shown in Algorithm 2.

Algorithm 2 CohCoSaMP

Input: sensing matrix $\boldsymbol{A}$, observations $\boldsymbol{y}$, conservative estimation of maximal degree $d_{\max}$, threshold value of estimation error ε, maximum iterations M

Output: estimated value $\hat{\boldsymbol{x}}$ of sparse vector $\boldsymbol{x}$

Initialize: residual $\boldsymbol{r}_0 = \boldsymbol{y}$, index set of sensing matrix column number $\Lambda_0 = \emptyset$, iteration $n = 1$ $\hat{\boldsymbol{x}} = \boldsymbol{0}$, $\Phi_n = \emptyset$

1. Calculate the coherence of each column with the two column corresponding to the phase angle and voltage magnitude variations. Obtain the two coefficient vectors of coherence as $\boldsymbol{u}_\theta = abs\left[\boldsymbol{A}_i^T \boldsymbol{A}_\theta\right]$, $\boldsymbol{u}_{\mathrm{U}} = abs\left[\boldsymbol{A}_i^T \boldsymbol{A}_{\mathrm{U}}\right]$.
2. Select the column indexes that have the largest $d_{\max} + 1$ values in $\boldsymbol{u}_\theta$ and $\boldsymbol{u}_{\mathrm{U}}$, and insert it into the set Φ_n. Update the index set Λ_n.

$$\Lambda_n = \Lambda_{n-1} \cup \Phi_n \tag{24}$$

3. Obtain the LSE solution $\hat{\boldsymbol{x}}_n$ using (21).
4. Update the residual using (22).
5. If $\|\boldsymbol{r}_n\|_2 < \varepsilon$, skip to step 9. Otherwise, if $n = 1$, select the column indexes that have the largest $2(d_{\max} + 1)$ values in $\boldsymbol{u}_\theta$ and $\boldsymbol{u}_{\mathrm{U}}$, and construct the set Φ_n with these indexes. Update index set Λ_n using (24), and return to step 3. Otherwise, set $n = n + 1$ and continue to step 6.
6. Calculate the inner product of the sensing matrix with residual as $\boldsymbol{u} = abs\left[\boldsymbol{A}^T \boldsymbol{r}_{n-1}\right]$. Construct Φ_n with the column indexes corresponding the largest $2(d_{\max} + 1)$ values in $\boldsymbol{u}$. Update index set Λ_n using (24).
7. Obtain the LSE solution $\hat{\boldsymbol{x}}_n$ using (21), and construct Φ_n with a column index corresponding to the largest $4(d_{\max} + 1)$ absolute values in $\hat{\boldsymbol{x}}_n$. Reconstruct the index set using (25). Update the residual using (26).

$$\Lambda_n = \Phi_n \tag{25}$$

$$\boldsymbol{r}_n = \boldsymbol{y} - \boldsymbol{A}_{\Lambda_n} \left(\boldsymbol{A}_{\Lambda_n}^T \boldsymbol{A}_{\Lambda_n} \right)^{-1} \boldsymbol{A}_{\Lambda_n}^T \boldsymbol{y} \tag{26}$$

8. Continue to step 9 if $n > M$ or $\|\boldsymbol{r}_n\|_2 < \varepsilon$; otherwise, set $n = n + 1$, and return to step 6.
9. Obtain the solution $\hat{\boldsymbol{x}}$ according to $\hat{\boldsymbol{x}}_n$ using (23).

where $\boldsymbol{A}_\theta$ denotes the submatrix of $\boldsymbol{A}$ that consists of the vectors of phase angle variations. $\boldsymbol{A}_\mathrm{U}$ denotes the submatrix of $\boldsymbol{A}$ that consists of the vectors of voltage magnitude variations.

Matrix $\tilde{\boldsymbol{J}}$ is formed after estimating the rows of each node via the proposed sparse-recovery algorithm. The estimation of the power flow Jacobian matrix $\hat{\boldsymbol{J}}$ is obtained by calculating the elements as shown in (27).

$$\hat{J}_{i,j} = \tilde{j}_{i,j} / \left\| \tilde{\boldsymbol{A}}_j \right\|_2 \tag{27}$$

By inverting the estimated power flow Jacobian matrix, the voltage-to-power sensitivity matrix is obtained.

IV. CASE STUDIES AND ANALYSIS

To verify the proposed algorithm, case studies on the IEEE 33-node test feeder are performed. The topology of the IEEE 33-node system is shown in Fig. 2 [38]. The rated voltage level is 12.66kV. Node 1 is the slack node. Nodes 2-33 are PQ nodes. The maximal degree of the network is 3. The rated capacity is 1MVA. Simulations are executed on a desktop with Intel Core i5-6500 3.20 GHz CPU, 8.00GB RAM and Windows 10 operating system.

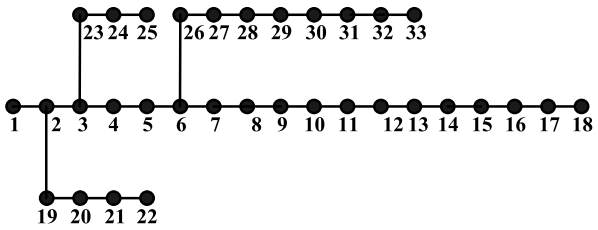

FIGURE 2. IEEE 33-node test feeder.

To simulate PMU measurements, equation (28) is used to generate the m^{th} actual active power of node i [21].

$$\dot{P}_i\left(t - m\Delta t\right) = \dot{P}_i(t) + \dot{P}_i(t) v_1^P \tag{28}$$

where $\dot{P}_i(t)$ denotes the current actual active power of node i, $\dot{P}_i\left(t - m\Delta t\right)$ is the m^{th} time step of actual active power, and v_1^P is a pseudorandom value drawn from the standard normal distribution to simulate the inherent fluctuations in load with zero mean and a standard deviation is 0.01.

The m^{th} historical active power of node i is calculated as shown in (29).

$$P_i\left(t - m\Delta t\right) = \dot{P}_i\left(t - m\Delta t\right) + v_2^P \tag{29}$$

v_2^P represents the random measurement noise. v_2^P is a pseudorandom values drawn from the standard normal distribution with a zero mean and a standard deviation of 0.025% [39].

Similarly, equation (30) and equation (31) are used to generate the m^{th} historical reactive power of node i.

$$\dot{Q}_i\left(t - m\Delta t\right) = \dot{Q}_i(t) + \dot{Q}_i(t) v_1^Q \tag{30}$$

$$Q_i\left(t - m\Delta t\right) = \dot{Q}_i\left(t - m\Delta t\right) + v_2^Q \tag{31}$$

where $\dot{Q}_i(t)$ denote the current actual reactive power of node i. $\dot{Q}_i\left(t - m\Delta t\right)$ is the m^{th} time step of actual reactive power. v_1^Q represents the pseudorandom value drawn from the standard normal distribution with zero mean and a standard deviation of 0.01. v_2^Q represents the random measurement noise. v_2^Q represents the pseudorandom value drawn from the standard normal distribution with zero mean and a standard deviation of 0.025%.

α is set as 0.001 to obtain the effective simulated active and reactive power measurements. The k^{th} historical phase angle and voltage magnitude are obtained by solving the power flow equation with the k^{th} active and reactive power that has already been generated.

Equation (32) is used to calculate the estimation error of the i^{th} row of the Jacobian matrix. Equations (33) and (34) are used to calculate the estimation errors of the power flow Jacobian matrix and voltage-to-power sensitivity matrix.

$$MSE_{\mathrm{J},i} = \frac{1}{K} \sum_{j=1}^{K} \left(\hat{J}_{i,j} - J_{i,j} \right)^2 \tag{32}$$

$$MSE_{\mathrm{J}} = \frac{1}{K^2} \sum_{j=1}^{K} \sum_{i=1}^{K} \left(\hat{J}_{i,j} - J_{i,j} \right)^2 \tag{33}$$

$$MSE_{\mathrm{S}} = \frac{1}{K^2} \sum_{j=1}^{K} \sum_{i=1}^{K} \left(\hat{Z}_{i,j} - Z_{i,j} \right)^2 \tag{34}$$

where $K = 2\left|\Omega_\mathrm{L}\right| + \left|\Omega_\mathrm{V}\right|$ denotes the dimension of the power flow Jacobian matrix and voltage-to-power sensitivity matrix. $\hat{J}_{i,j}$ and $\hat{Z}_{i,j}$ denote the estimation values, and $J_{i,j}$ and $Z_{i,j}$ are the theoretical values. Error tolerance ε is set as 0.1% of the l_2 norm of the corresponding active and reactive power measurement variations in estimation.

A. CONVERGENCE OF THE ALGORITHM

For IEEE 33-node test feeder, the power flow Jacobian matrix is of 64 dimensions. More than 64 measurement groups are required for LSE method. Therefore, the number of measurement groups is set as 30, 35, 40, 45, 50, 55 and 60. The conservative estimation of the maximal degree of the distribution network is set as 4. LSE, OMP, ROMP, CoSaMP and the proposed CohCoSaMP are applied to solve the problem. When the estimation error is less than 1, the i^{th} row is treated as successfully estimated. Table 1 shows the number of rows of the Jacobian matrix that fail to be estimated with the various algorithms. It is necessary to have more valid measurements than the dimension of the Jacobian matrix for the LSE to form the overdetermined equation, which means that LSE cannot estimate the Jacobian matrix as long as the number of measurements is less than 64, as shown in Table 1. OMP, ROMP, and CoSaMP can estimate several lines of the

TABLE 1. Number of rows for which estimation failed.

Measurement groups	30	35	40	45	50	55	60
LS	64	64	64	64	64	64	64
OMP	52	52	45	42	35	25	17
ROMP	51	48	38	38	31	24	15
CoSaMP	58	49	40	21	26	14	8
CohCoSaMP	2	1	0	0	0	0	0

Jacobian matrix. As the number of measurements increases, the number of successfully estimated lines in the Jacobian matrix also increases. However, these algorithms are unable to estimate the entire Jacobian matrix even if the number of measurements increases to 60. In contrast, CohCoSaMP can estimate the entire Jacobian matrix when the number of measurements is greater than 40.

The first 32 values of the 6^{th} row of the Jacobian matrix estimated by OMP, ROMP, CoSaMP, and CohCoSaMP with 40 measurement groups are listed in Table 2. The corresponding theoretical values are shown in the last column of Table 2. In contrast to CohCoSaMP, the algorithm OMP, ROMP, and CoSaMP cannot find the exact columns with the nonzero elements of Jacobian matrix (shown in gray in Table 2), and their estimation values deviate greatly from the theoretical values.

TABLE 2. Estimation values with various methods of 6^{th} row.

Column number	OMP	ROMP	CoSaMP	CohCoSaMP	Theoretical value
1	-977.45	0.00	0.00	0.00	0.00
2	197.36	0.00	0.00	0.00	0.00
3	157.13	0.00	0.00	0.00	0.00
4	0.00	0.00	0.00	0.00	0.00
5	0.00	0.00	1593.12	212.87	212.95
6	-166.68	-82.91	-587.45	-272.55	-272.62
7	67.10	-29.21	0.00	59.63	59.67
8	0.00	145.92	622.88	0.02	0.00
9	0.00	-65.22	0.00	0.00	0.00
10	0.00	0.00	-983.80	0.00	0.00
11	118.86	0.00	1108.41	0.00	0.00
12	-303.99	0.00	-575.18	0.00	0.00
13	204.21	0.00	1628.21	0.00	0.00
14	0.00	0.00	-2763.99	0.00	0.00
15	0.00	0.00	1476.10	0.00	0.00
16	0.00	0.00	649.70	0.00	0.00
17	-8.76	0.00	-625.51	0.00	0.00
18	115.82	0.00	0.00	0.00	0.00
19	-56.21	0.00	0.00	0.00	0.00
20	0.03	0.00	0.00	0.00	0.00
21	49.60	0.00	0.00	0.00	0.00
22	-141.59	0.00	0.00	0.00	0.00
23	51.09	0.00	0.00	0.00	0.00
24	-20.95	1.32	0.00	0.00	0.00
25	0.00	0.00	-2957.28	0.03	0.00
26	20.78	0.00	1709.16	0.00	0.00
27	0.00	0.00	0.00	0.00	0.00
28	0.00	82.86	0.00	0.00	0.00
29	17.88	-85.81	0.00	0.00	0.00
30	16.97	58.80	0.00	0.00	0.00
31	0.00	31.31	-533.35	0.00	0.00
32	-26.47	-64.64	337.77	0.00	0.00

Table 3 shows the coherence rank of phase angle variation of each node. The table cells filled with orange are the node IDs that are directly connected to the corresponding node. As shown in Table 3, for most nodes their directly connected nodes rank in top 7. Therefore, the column number of the sensing matrix corresponding to the directly connected nodes can be selected into the index set after coherence evaluation for most of the nodes. Moreover, for other nodes, a better index set is initialized for the CoSaMP process that will promote the efficiency of the recovery algorithm.

TABLE 3. Coherence rank of phase angle variations of each node.

Node ID	1	2	3	4	5	6	7	…	24	…
2	2	3	4	5	23	19	6	…	25	…
3	3	2	4	5	23	6	26	…	25	…
4	4	5	3	6	26	26	27	…	15	…
5	5	4	26	27	6	28	29	…	15	…
6	6	26	27	5	7	28	8	…	19	…
7	7	8	6	26	9	27	5	…	17	…
8	8	7	9	6	10	11	26	…	17	…
9	9	10	11	8	12	7	13	…	33	…
10	10	11	12	9	13	8	14	…	32	…
11	11	10	12	9	13	14	8	…	32	…
12	12	11	10	13	9	14	15	…	32	…
13	13	14	15	16	12	11	10	…	33	…
14	14	15	13	16	17	18	12	…	33	…
15	15	16	14	13	17	18	12	…	33	…
16	16	15	14	17	18	13	12	…	33	…
17	17	18	16	15	14	13	12	…	33	…
18	18	17	16	15	14	13	12	…	33	…
19	19	2	3	4	5	5	27	…	20	…
20	20	21	22	19	2	23	24	…	10	…
21	21	20	22	19	2	24	23	…	10	…
22	22	21	20	19	2	24	23	…	16	…
23	23	3	24	2	4	4	19	…	13	…
24	24	25	23	3	2	19	4	…	13	…
25	25	24	23	3	2	19	4	…	33	…
26	26	6	27	5	28	7	29	…	16	…
27	27	26	6	28	5	29	30	…	16	…
28	28	29	30	27	31	32	33	…	15	…
29	29	30	28	31	32	33	27	…	15	…
30	30	29	31	28	32	33	27	…	15	…
31	31	32	33	30	29	28	27	…	15	…
32	32	33	31	29	30	28	27	…	15	…
33	33	32	31	29	30	28	27	…	15	…

B. COMPUTATIONAL EFFICIENCY

To ensure the effectiveness of the comparison, more measurement groups are needed for successful estimation with the exiting methods. The number of measurement groups is set as 100, 150, 200, 250, 300, 350 and 400. The conservative estimation of maximal degree is set as 4. For each type of group, 10 times of estimations are performed to obtain the average error of estimation of the power flow Jacobian matrix and the voltage-to-power sensitivity matrix shown in Table 4, Fig. 3 and Table 5, Fig. 4, respectively. The accuracy of OMP is the lowest; the accuracy of ROMP is higher. CoSaMP cannot achieve estimation because of the coherence between the columns of the sensing matrix, which makes it challenging to find the directly connected nodes with a limited size of the index set. In contrast, CohCoSaMP not only realizes the

TABLE 4. Average error of the power flow Jacobian matrix ($\times 10^{-4}$).

Measurement groups	100	150	200	250	300	350	400
OMP	161	67.5	86.9	63.3	45.0	28.7	31.3
ROMP	130	54.4	49.9	42.0	31.4	18.9	18.2
CoSaMP	-	-	-	-	-	-	-
CohCoSaMP	5.87	5.00	4.52	4.41	3.67	3.61	3.26

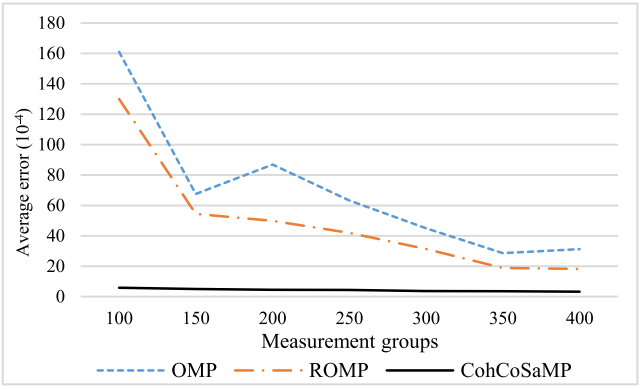

FIGURE 3. Average error of the power flow Jacobian matrix.

TABLE 5. Average error of the voltage-to-power sensitivity matrix ($\times 10^{-12}$).

Measurement groups	100	150	200	250	300	350	400
OMP	439	219	197	119	108	66.8	78.7
ROMP	362	170	132	100	74.3	55.8	61.6
CoSaMP	-	-	-	-	-	-	-
CohCoSaMP	26.8	16.2	16.4	13.8	12.1	10.9	8.95

estimation of the Jacobian matrix but also greatly improve the accuracy.

Table 6 and Table 7 show the average iterations and average computation time, respectively, for each algorithm. With the increase in measurements, the iterations and computation time greatly increase for OMP. The iterations and computation time of ROMP do not increase substantially for increasing measurements, but large number of iterations are still needed to find the optimal solution. Notably, relative to other algorithms, CohCoSaMP can find the optimal solution with fewer iterations and can reduce the computation time greatly to achieve a correlation evaluation, making this approach more suitable for online application.

C. ESTIMATION ACCURACY

First, the number of measurement groups is set as 30, 35, 40, 45, 50, 55 and 60. The conservative estimation of maximal degree is set as 4. CohCoSaMP is used to solve the sparsity-recovery problem. The estimation errors are shown in Table 8. Then, the number of measurement groups is set as 100, 500, 1000, 1500 and 2000. LSE is used to solve the problem. The estimation errors are shown in Table 9. When the number of measurement groups is 60, CohCoSaMP has a higher accuracy than LSE with a measurement number of 1500 and almost the same accuracy when the measurement number is 2000. Therefore, CohCoSaMP can ensure accurate estimation and simultaneously reduce the dependence on the number of measurements by a considerable degree.

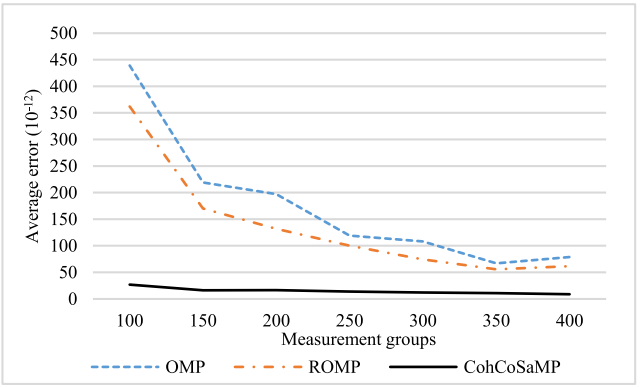

FIGURE 4. Average error of the voltage-to-power sensitivity.

TABLE 6. Average iterations ($\times 10^2$).

Measurement groups	100	150	200	250	300	350	400
OMP	30.6	29.2	45.0	65.0	89.9	98.1	110
ROMP	3.25	3.30	3.34	3.62	3.90	3.99	4.19
CohCoSaMP	0.73	0.74	0.73	0.74	0.74	0.74	0.74

TABLE 7. Average computation time (s).

Measurement groups	100	150	200	250	300	350	400
OMP	0.62	0.66	1.28	2.19	3.42	4.21	5.49
ROMP	0.08	0.08	0.09	0.10	0.11	0.11	0.13
CohCoSaMP	0.01	0.01	0.01	0.02	0.01	0.01	0.02

TABLE 8. Estimation errors of the Jacobian matrix ($\times 10^{-4}$).

Measurement groups	40	45	50	55	60
CohCoSaMP	10.7	12.4	9.33	8.45	7.41

TABLE 9. Estimation errors of the voltage-to-power sensitivity matrix ($\times 10^{-4}$).

Measurement groups	100	500	1000	1500	2000
LSE	587	17.5	15.9	12.3	6.95

V. CONCLUSION

We have presented an online method to estimate the voltage-to-power sensitivity for smart distribution networks based on

PMU measurements considering the sparsity of the power flow Jacobian matrix. Using the sparsity of the power flow Jacobian matrix, compressive sensing is used to transform the estimation problem into a sparse-recovery problem that enables estimation with fewer measurements. Furthermore, the performance of the existing sparse-recovery algorithm is improved using the coherence between the vectors of phase angle and voltage magnitude variations of the directly connected nodes. The proposed algorithm greatly increases the success rate of estimation and improves the estimation accuracy. To realize the estimation of the power flow Jacobian matrix, PMU must be equipped in each node of the distribution network, which may not be economic affordable. Planned further research will focus on estimating the equivalent voltage sensitivities with fewer PMUs equipped in the key nodes of the distribution network.

REFERENCES

[1] J. J. Nielsen *et al.*, "Secure real-time monitoring and management of smart distribution grid using shared cellular networks," *IEEE Wireless Commun.*, vol. 24, no. 2, pp. 10–17, Apr. 2017.

[2] X. Hu, C. Zou, C. Zhang, and Y. Li, "Technological developments in batteries: A survey of principal roles, types, and management needs," *IEEE Power Energy Mag.*, vol. 15, no. 5, pp. 20–31, Sep./Oct. 2017.

[3] P. Li *et al.*, "Coordinated control method of voltage and reactive power for active distribution networks based on soft open point," *IEEE Trans. Sustain. Energy*, vol. 8, no. 4, pp. 1430–1442, Oct. 2017.

[4] F. Zare, H. Soltani, D. Kumar, P. Davari, H. A. M. Delpino, and F. Blaabjerg, "Harmonic emissions of three-phase diode rectifiers in distribution networks," *IEEE Access*, vol. 5, pp. 2819–2833, Feb. 2017.

[5] H. Xing and X. Sun, "Distributed generation locating and sizing in active distribution network considering network reconfiguration," *IEEE Access*, vol. 5, pp. 14768–14774, Jul. 2017.

[6] A. Giannitrapani, S. Paoletti, A. Vicino, and D. Zarrilli, "Optimal allocation of energy storage systems for voltage control in LV distribution networks," *IEEE Trans. Smart Grid*, vol. 8, no. 6, pp. 2859–2870, Nov. 2017.

[7] I. K. Song, W. W. Jung, J. Y. Kim, S. Y. Yun, J. H. Choi, and S. J. Ahn, "Operation schemes of smart distribution networks with distributed energy resources for loss reduction and service restoration," *IEEE Trans. Smart Grid*, vol. 4, no. 1, pp. 367–374, Mar. 2013.

[8] A. Garces, "A linear three-phase load flow for power distribution systems," *IEEE Trans. Power Syst.*, vol. 31, no. 1, pp. 827–828, Jan. 2016.

[9] K. H. Youssef, "A new method for online sensitivity-based distributed voltage control and short circuit analysis of unbalanced distribution feeders," *IEEE Trans. Smart Grid*, vol. 6, no. 3, pp. 1253–1260, May 2015.

[10] K. E. Van Horn, A. D. Domínguez-García, and P. W. Sauer, "Measurement-based real-time security-constrained economic dispatch," *IEEE Trans. Power Syst.*, vol. 31, no. 5, pp. 3548–3560, Sep. 2016.

[11] E. M. Stewart, S. Kiliccote, C. M. Shand, A. W. McMorran, R. Arghandeh, and A. von Meier, "Addressing the challenges for integrating micro-synchrophasor data with operational system applications," in *Proc. IEEE PES General Meeting*, Jul. 2014 pp. 1–5.

[12] A. G. Phadke and J. S. Thorp, *Synchronized Phasor Measurements and Their Applications*. New York, NY, USA: Springer, 2008, pp. 29–48.

[13] R. Pourramezan, Y. Seyedi, H. Karimi, G. Zhu, and M. Mont-Briant, "Design of an advanced phasor data concentrator for monitoring of distributed energy resources in smart microgrids," *IEEE Trans. Ind. Informat.*, vol. 13, no. 6, pp. 3027–3036, Dec. 2017.

[14] A. von Meier, E. Stewart, A. McEachern, M. Andersen, and L. Mehrmanesh, "Precision micro-synchrophasors for distribution systems: A summary of applications," *IEEE Trans. Smart Grid*, vol. 8, no. 6, pp. 2926–2936, Nov. 2017.

[15] A. von Meier, D. Culler, A. McEachern, and R. Arghandeh, "Micro-synchrophasors for distribution systems," in *Proc. IEEE Power Energy Soc. Innov. Smart Grid Technol. Conf.*, Feb. 2014, pp. 1–5.

[16] Y. Chakhchoukh, V. Vittal, and G. T. Heydt, "PMU based state estimation by integrating correlation," *IEEE Trans. Power Syst.*, vol. 29, no. 2, pp. 617–626, Mar. 2014.

[17] M. Asprou and E. Kyriakides, "Identification and estimation of erroneous transmission line parameters using PMU measurements," *IEEE Trans. Power Del.*, vol. 32, no. 6, pp. 2510–2519, Dec. 2017.

[18] K. Dasgupta and S. A. Soman, "Line parameter estimation using phasor measurements by the total least squares approach," in *Proc. IEEE Power Energy Soc. General Meeting*, Jul. 2013, pp. 1–5.

[19] J. Zhang, X. Zheng, Z. Wang, L. Guan, and C. Y. Chung, "Power system sensitivity identification—Inherent system properties and data quality," *IEEE Trans. Power Syst.*, vol. 32, no. 4, pp. 2756–2766, Jul. 2017.

[20] X. Wang, J. W. Bialek, and K. Turitsyn, "PMU-based estimation of dynamic state Jacobian matrix and dynamic system state matrix in ambient conditions," *IEEE Trans. Power Syst.*, vol. 33, no. 1, pp. 681–690, Jan. 2018.

[21] Y. C. Chen, A. D. Domínguez-García, and P. W. Sauer, "Measurement-based estimation of linear sensitivity distribution factors and applications," *IEEE Trans. Power Syst.*, vol. 29, no. 3, pp. 1372–1382, May 2014.

[22] M. Saadeh, R. McCann, M. Alsarray, and O. Saadeh, "A new approach for evaluation of the bus admittance matrix from synchrophasors: (A statistical Ybus estimation approach)," *Int. J. Electr. Power Energy Syst.*, vol. 93, pp. 395–405, Dec. 2017.

[23] Y. C. Chen, J. Wang, A. D. Domínguez-García, and P. W. Sauer, "Measurement-based estimation of the power flow Jacobian matrix," *IEEE Trans. Smart Grid*, vol. 7, no. 5, pp. 2507–2515, Sep. 2016.

[24] Y. C. Chen, A. D. Domínguez-García, and P. W. Sauer, "A sparse representation approach to online estimation of power system distribution factors," *IEEE Trans. Power Syst.*, vol. 30, no. 4, pp. 1727–1738, Jul. 2015.

[25] M. Babakmehr, M. Simões, M. Wakin, and F. Harirchi, "Compressive sensing-based topology identification for smart grids," *IEEE Trans. Ind. Informat.*, vol. 12, no. 2, pp. 532–543, Apr. 2016.

[26] E. J. Candès, J. Romberg, and T. Tao, "Robust uncertainty principles: Exact signal reconstruction from highly incomplete frequency information," *IEEE Trans. Inf. Theory*, vol. 52, no. 2, pp. 489–509, Feb. 2006.

[27] W. Huang, Y. Huang, W. Xu, and L. Yang, "Beam-blocked channel estimation for FDD massive MIMO with compressed feedback," *IEEE Access*, vol. 5, pp. 11791–11804, 2017.

[28] A. Fannjiang and W. Liao, "Coherence pattern–guided compressive sensing with unresolved grids," *SIAM J. Imag. Sci.*, vol. 5, no. 1, pp. 179–202, 2012.

[29] Y. Weng, Y. Liao, and R. Rajagopal, "Distributed energy resources topology identification via graphical modeling," *IEEE Trans. Power Syst.*, vol. 32, no. 4, pp. 2682–2694, Jul. 2017.

[30] A. Armenia and J. H. Chow, "A flexible phasor data concentrator design leveraging existing software technologies," *IEEE Trans. Smart Grid*, vol. 1, no. 1, pp. 73–81, Jun. 2010.

[31] C. Ekanadham, D. Tranchina, and E. P. Simoncelli, "Recovery of sparse translation-invariant signals with continuous basis pursuit," *IEEE Trans. Signal Process.*, vol. 59, no. 10, pp. 4735–4744, Oct. 2011.

[32] J. A. Tropp and A. C. Gilbert, "Signal recovery from random measurements via orthogonal matching pursuit," *IEEE Trans. Inf. Theory*, vol. 53, no. 12, pp. 4655–4666, Dec. 2007.

[33] T. Liu T. Qiu, R. Dai, J. Li, L. Chang, and R. Li, "Nonlinear regression A*OMP for compressive sensing signal reconstruction," *Digit. Signal Process.*, vol. 69, pp. 11–21, Oct. 2017.

[34] J. A. Tropp, "Greed is good: Algorithmic results for sparse approximation," *IEEE Trans. Inf. Theory*, vol. 50, no. 10, pp. 2231–2242, Oct. 2004.

[35] D. Needell and R. Vershynin, "Signal recovery from incomplete and inaccurate measurements via regularized orthogonal matching pursuit," *IEEE J. Sel. Topics Signal Process.*, vol. 4, no. 2, pp. 310–316, Apr. 2010.

[36] D. Needell and J. A. Tropp, "CoSaMP: Iterative signal recovery from incomplete and inaccurate samples," *Appl. Comput. Harmon. Anal.*, vol. 26, no. 3, pp. 301–321, May 2008.

[37] E. J. Candés and J. Romberg. (2005). *ℓ_1-MAGIC: Recovery of Sparse Signals via Convex Programming*. [Online]. Available: http://www.acm.caltech.edu/l1magic

[38] M. E. Baran and F. F. Wu, "Optimal capacitor placement on radial distribution systems," *IEEE Trans. Power Del.*, vol. 4, no. 1, pp. 725–734, Jan. 1989.

[39] R. Arghandeh, M. Gahr, A. von Meier, G. Cavraro, M. Ruh, and G. Andersson, "Topology detection in microgrids with micro-synchrophasors," in *Proc. IEEE PES General Meeting*, Jul. 2015, pp. 1–5.

PENG LI (M'11) was born in Tianjin, China, in 1981. He received the B.S. and Ph.D. degrees in electrical engineering from Tianjin University, Tianjin, China, in 2004 and 2010, respectively. He is currently an Associate Professor with the School of Electrical and Information Engineering, Tianjin University. His current research interests include distributed generation system and microgrids, smart distribution system, active distribution network, and transient simulation and analysis.

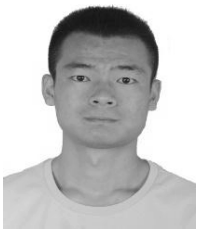

HONGZHI SU was born in Jianping, Liaoning, China, in 1990. He received the B.S. degree in electrical engineering from Tianjin University, Tianjin, China, in 2013. He is currently pursuing the Ph.D. degree with the School of Electrical and Information Engineering, Tianjin University. His current research interests include smart distribution system analysis, monitoring, and control.

CHENGSHAN WANG (SM'11) was born in Tianjin, China, in 1962. He received the Ph.D. degree in electrical engineering from Tianjin University, Tianjin, China, in 1991. From 1994 to 1996, he was a Senior Academic Visitor with Cornell University, Ithaca, NY, USA. From 2001 to 2002, he was a Visiting Professor with Carnegie Mellon University, Pittsburgh, PA, USA. He is currently a Professor with the School of Electrical and Information Engineering, Tianjin University. He is also the Director of the Key Laboratory of Smart Grid of Ministry of Education, Tianjin University. His current research interests include distribution system analysis and planning, distributed generation system and microgrid, and power system security analysis.

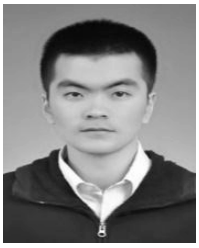

ZHELIN LIU was born in Jiangxi, China, in 1991. He received the B.S. and M.Sc. degrees in electrical engineering from Tianjin University, Tianjin, China, in 2013 and 2016, respectively, where he is currently pursuing the Ph.D. degree with the School of Electrical and Information Engineering, Tianjin University. His current research interests include distribution system state estimation.

JIANZHONG WU (M'14) received the Ph.D. degree from Tianjin University, Tianjin, China, in 2004. From 2004 to 2006, he was with Tianjin University, where he is currently an Associate Professor. From 2006 to 2008, he was a Research Fellow with the University of Manchester, Manchester, U.K. He is currently a Professor with the School of Engineering, Institute of Energy, Cardiff University, Cardiff, U.K. His current research interests include energy infrastructure and smart grids. He is a member of the Institution of Engineering and Technology and the Association for Computing Machinery.